

Nanocrystals formation and intense green emission in thermally annealed AlN:Ho films for microlaser cavities and photonic applications

Muhammad Maqbool, Ghafar Ali, Sung Oh Cho, Iftikhar Ahmad, Mazhar Mehmood et al.

Citation: *J. Appl. Phys.* **108**, 043528 (2010); doi: 10.1063/1.3478770

View online: <http://dx.doi.org/10.1063/1.3478770>

View Table of Contents: <http://jap.aip.org/resource/1/JAPIAU/v108/i4>

Published by the [American Institute of Physics](#).

Additional information on J. Appl. Phys.

Journal Homepage: <http://jap.aip.org/>

Journal Information: http://jap.aip.org/about/about_the_journal

Top downloads: http://jap.aip.org/features/most_downloaded

Information for Authors: <http://jap.aip.org/authors>

ADVERTISEMENT



AIPAdvances

Now Indexed in Thomson Reuters Databases

Explore AIP's open access journal:

- Rapid publication
- Article-level metrics
- Post-publication rating and commenting

Nanocrystals formation and intense green emission in thermally annealed AlN:Ho films for microlaser cavities and photonic applications

Muhammad Maqbool,^{1,a)} Ghafar Ali,² Sung Oh Cho,² Iftikhar Ahmad,³ Mazhar Mehmood,⁴ and Martin E. Kordesch⁵

¹*Department of Physics and Astronomy, Ball State University, Muncie, Indiana 47306, USA*

²*Department of Nuclear and Quantum Engineering, KAIST, Daejeon, South Korea*

³*Department of Physics, Hazara University, Mansehra, NWFP, Pakistan*

⁴*National Center for Nanotechnology, Pakistan Institute of Engineering and Applied Sciences, Islamabad, Pakistan*

⁵*Department of Physics and Astronomy, Ohio University, Athens, Ohio 45701, USA*

(Received 28 April 2010; accepted 17 July 2010; published online 27 August 2010)

Plasma magnetron sputtered thin films of AlN:Ho deposited on flat silicon substrates and optical fiber were characterized and analyzed for structural changes after thermal annealing at 1173 K for 40 min, by atomic force microscopy (AFM). The films grown, at liquid nitrogen temperature, on silicon substrates were amorphous while those deposited around optical fiber were crystalline. The films were also investigated for any change in the luminescence when thermal activation was performed for 40 min in a nitrogen atmosphere. The AFM analysis identified the existence of crystalline structures in parts of the films after thermal annealing. The x-ray diffraction could not provide those results. The films around optical fiber were crystalline even deposited at liquid nitrogen temperature. Clearly, amorphous films are hard to achieve on smaller substrate size. Direct observation of green emission is possible with naked eye, when the thermally annealed films are studied under cathodoluminescence. The green emission occurs at 549 nm as a result from $^5S_2 \rightarrow ^5I_8$ transition in Ho^{3+} that enhanced with thermal activation, making it a very useful candidate for photonic and optical devices applications. © 2010 American Institute of Physics. [doi:10.1063/1.3478770]

I. INTRODUCTION

Rare-earth-doped III-nitride semiconductor thin films are attracting increasing attention as phosphor materials for use in optical displays. Recent progress toward nitride-based light-emitting diode and electroluminescent devices has been made using crystalline and amorphous GaN and AlN doped with a variety of rare-earth elements.^{1–15} The electronic structure of the rare-earth ions differ from the other elements and are characterized by an incompletely filled $4f^n$ shell. The $4f$ electrons lay inside the ion and are shielded from the surroundings by the filled $5s^2$ and $5p^6$ electron orbital.¹⁶ When these materials are excited by various means, intense sharp-line emission is observed due to intra- $4f^n$ -shells transitions of the rare-earth ion core.^{15,17–19}

The amorphous III-nitride semiconductors are equally important like their crystalline counterpart because the amorphous material can be grown at room temperature with little stress due to lattice mismatch.^{5,15,19} They may also be more suitable for waveguides and cylindrical and spherical laser cavities because of the elimination of grain boundaries at low temperature growth.^{1–6,20,21} High thermal conductivity, stability, and chemical inertness of AlN also make very useful for its electrical, optical, and thermal applications.^{22,23} AlN is a better host than other nitrides family due to its wide band-gap of 210 nm, making it transparent to a wide range of

visible, UV, and IR emissions. Thus, if doped with a rare-earth element, it can be used for a number of applications.^{1,2,24,25}

II. EXPERIMENTAL DETAILS

Then films of AlN:Ho were prepared at room temperature and 77 K by rf magnetron sputtering of an aluminum–holmium bimetal target in a pure nitrogen atmosphere in a cryopumped vacuum system. The aluminum–holmium bimetal target was made by drilling a hole (1/4 in. diameter) in the aluminum target (2 in. diameter) and placing a circular disk of 99.99% pure holmium in the hole. Holmium was then cosputtered with aluminum. The background vacuum in the chamber was $<3 \times 10^{-5}$ Torr. All the films were deposited on silicon (100) substrates and optical fibers with diameters ranging from 10 to 80 μm . Nitrogen pressures between 5 and 8 mTorr was used in the entire work. Liquid nitrogen was used for cooling the substrates during low temperature deposition of films. Films of different thickness were grown on both types of substrates ranging from 150 nm up to 10 μm on fibers and up to 1 μm on flat silicon substrates. These thicknesses were measured with a quartz crystal thickness monitor in the growth chamber, a transmission IR microscope and scanning electron microscope (SEM). X-rays diffraction (XRD), SEM, and atomic force microscopy (AFM) were used to determine and analyze the structure of the films. The fibers of 50 mm length were clamped to the liquid nitrogen reservoir along their length, with the last 10 mm extending beyond the cooling clamp. No measurement

^{a)}Electronic mail: mmaqbool@bsu.edu.

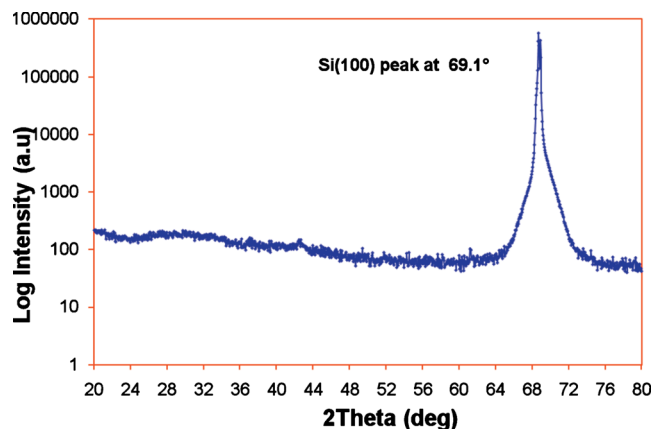


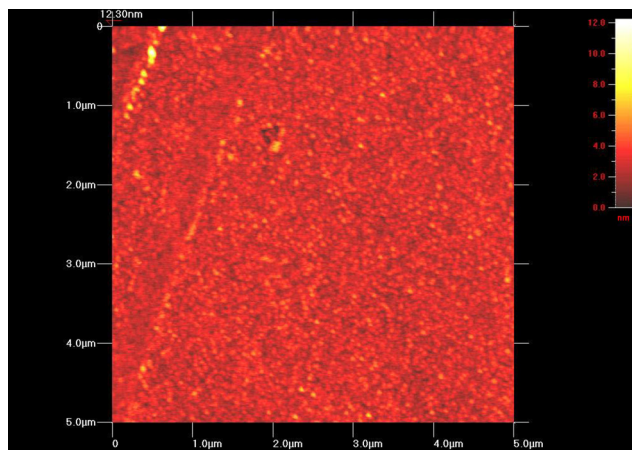
FIG. 1. (Color online) XRD analysis of the AlN:Ho films deposited on Si(100) substrates.

of the fiber tip temperature during deposition was made. The structure of the as-deposited and thermally annealed films on silicon substrate were analyzed by XRD. No diffraction peaks were observed, indicating that the films are amorphous. However AFM results indicate the existence of small nanocrystals in the amorphous films.

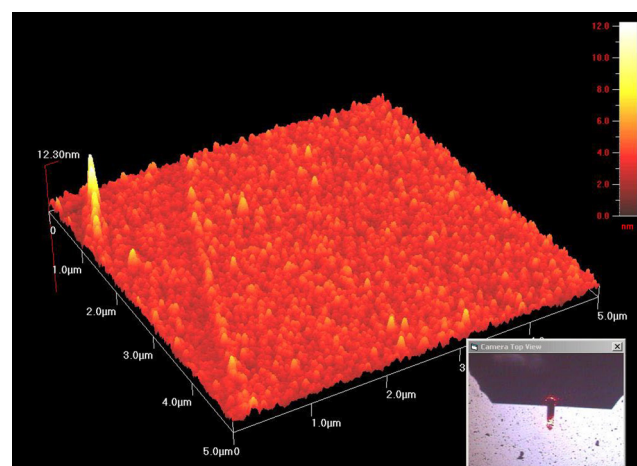
III. RESULTS AND DISCUSSION

Figure 1 shows the XRD analysis of the thermally annealed AlN:Ho films deposited on flat Si(100) substrate. Only one peak can be observed in the film at 69.1° which corresponds to Si(100). No other peak is present in the figure, indicating that the films deposited on flat silicon substrates are amorphous. Thermal activation of the films at 1173 K has not changed the structure of the films. Glancing angle XRD analysis also revealed the same results.

Figure 2 shows the AFM results of the as-deposited amorphous and thermally annealed films. Figure 2(a) shows the two-dimensional (2D) picture of the films annealed at 1173 K. The columns of the atoms in a sequence on the left side of the image show the crystal formation in the film. The crystal formation is very strong in a region of $1\ \mu\text{m}$. However, longer crystal structure is also found extending to a size of $4\ \mu\text{m}$. The crystal size is found to be about 0.5 nm. Annealing at 1173 K results in the formation of new AlN crystals. These results are very interesting and need further discussion. The formation of crystals in amorphous AlN:Ho films with thermal annealing is observed under AFM analysis. However, XRD results did not provide any information of such crystals formation in an amorphous matrix. The annealing at 1173 K in nitrogen atmosphere for 40 min results in formation of new small crystallites in initially mostly amorphous AlN. The material becomes crystalline and AFM images show that transformation to the crystalline state is not complete. The transformation from amorphous to crystalline is complicated because not only Al and N but also oxygen contaminants substitute the nitrogen atoms sometimes. The contaminant O atoms rearrange themselves during annealing. We can speculate that annealing induces new defects, like nitrogen or aluminum vacancies and aluminum interstitials (these defects are reasonable in a sample with predominantly crystalline phase).



(a)



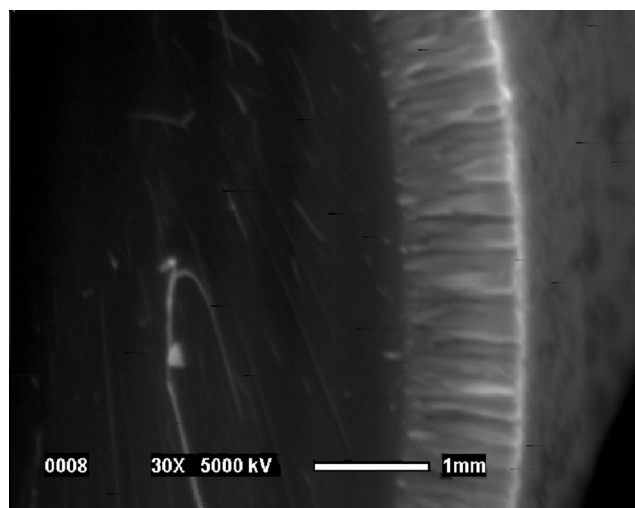
(b)

FIG. 2. (Color online) 2D and three-dimensional AFM image of crystal formation in an amorphous matrix of AlN:Ho.

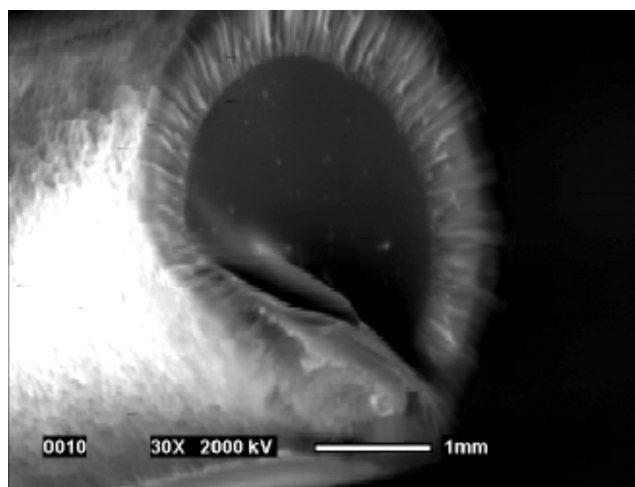
Figure 3 shows the cross-sectional image of the AlN:Ho films deposited around optical fibers. The diameter of the fiber was $80\ \mu\text{m}$. Figure 3(a) gives a close look of the right side of the fiber while Fig. 3(b) represents cross-sectional image of the entire fiber. The central dark circle shows the optical fiber and the circular disk around the fiber is the AlN:Ho film. A small section in the bottom of the Fig. 3(b) shows some damage to that part of the film while working with it. The granular lines indicate that the films around the fibers are crystalline.

Figure 4 gives a diagrammatical view of cylindrical and ring microlasers cavities in waveguide mode (WM) and whispering gallery mode (WGM). The central dark region shows a cross-sectional view of fiber while the disk around the fiber represents thin film optical material deposited around the fiber. It is clear from the figure that if the thickness of the film is very small then light, once enters into the film cannot proceed around the fiber without hitting it. This prevents the WGM propagation of light and develops laser cavity in WM.

The results obtained in Figs. 3 and 4 are very useful for lasers and other optical devices applications. Figure 3 in-



(a)



(b)

FIG. 3. Cross-sectional images of AlN:Ho films deposited around fiber.

forms that the films deposited on optical fibers are crystalline even if they are deposited at liquid nitrogen temperature. Though we were unable to measure the temperature of the tip of the fiber during the film growth process but still we believe that it was close to liquid nitrogen temperature. The diameter of the optical fiber was $80\ \mu\text{m}$. Thus we can very easily extract an important physics from our results. That is “smaller is the size of fiber or substrate harder to get an amorphous film.” Thus a crystalline film can be easily obtained if we deposit film on small size substrates or fibers. Another goal of this work was to deposit amorphous films around optical fiber to construct cylindrical and ring laser cavities in optical fibers in WM and WGM. Cylindrical and ring microlaser are already produced by depositing some organic liquids on optical fibers.^{26,27} However, we want to produce ring and cylindrical microlasers in rare-earth doped in nitride semiconductors (AlN). To produce these lasers in WM and WGM we need to choose and deposit an appropriate thin film around the fiber where the light propagation occur without any major loss. The presence of grain bound-

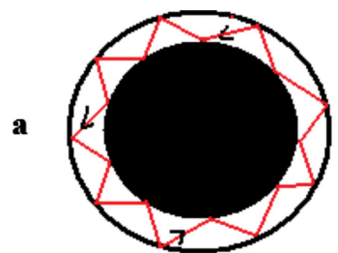
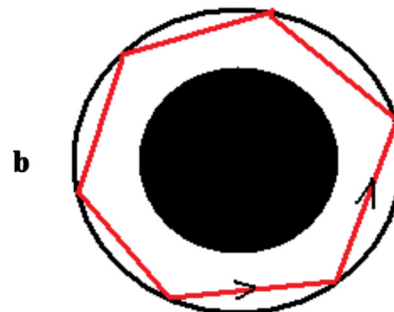
**Waveguide Mode****Whispering Gallery Mode**

FIG. 4. (Color online) Cylindrical and ring microlaser cavities in (a) WM and (b) WGM.

aries in crystalline films around optical fibers will create scattering centers which will ultimately block the propagation of light in the film around the fiber. Thus, in order to produce microlasers in transition metals doped in nitride semiconductors around optical fibers the deposited films must be amorphous.^{26,27} Moreover, to achieve these lasers in WGM, the thickness of the deposited films around optical fiber must be greater than one-fifth ($1/5$) of the diameter of the fiber. Any film with thickness smaller than the mentioned value could be suitable for microlasers in WM but not in WGM.^{26,27} In case of the WGM the light propagation is independent of the fiber, however in WM the propagation of light depends upon the nature of the fiber because reflection of light from the fiber will occur. Such laser cavities in WM and WGM are produce and reported in some polymers by Vardeny.^{26,27} We are in the process to produce these lasers in rare-earth doped nitride semiconductors. Thus we can construct cylindrical and ring microlaser cavities in AlN:Ho films but we must overcome the crystalline structure of the films around the fibers. One way to achieve this goal is to use a thin films deposition system where the growth rate is faster than the one we have used. In that was the deposition time will be short and hence the liquid nitrogen will be able to keep the films amorphous before the temperature starts rising and the crystal growth appears. Another way is to use optical fibers of smaller diameters and films less thick than the current thickness. In this way one cannot only maintain the one-fifth ratio of the film thickness to the fiber diameter but also will be able to deposit those films in short time keeping them amorphous. Fortunately, we have already produced smaller diameter optical fibers by pulling the thicker fibers in a fire

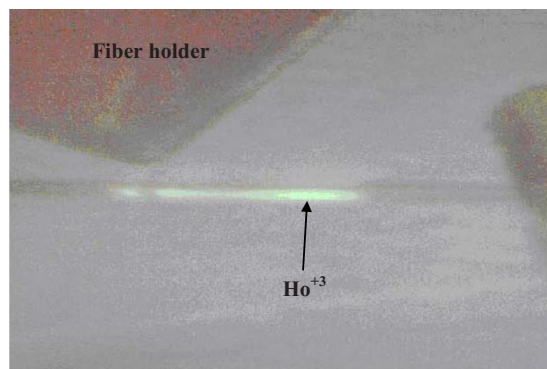


FIG. 5. (Color online) Light emission from thermally annealed AlN:Ho deposited around optical fiber.

flame. We are in the process of repeating our experiments and the results will be published once successful in getting these microlasers.

Figure 5 gives a direct observation of the green emission from the thermally annealed AlN:Ho film deposited around optical fiber of 80 μm diameter. The picture was taken by a digital camera when the fiber with the deposited film around it was under electron excitation in cathodoluminescence equipment. We were unable to see the green emission with naked eye from the same fiber placed under the same conditions in cathodoluminescence before thermal annealing. We have already reported the green emission at 549 nm from AlN:Ho films as a result of $^5S_2 \rightarrow ^5I_8$ transition.²⁴

Figure 6 shows cathodoluminescence emission spectra of the as-deposited AlN:Ho and the thermally annealed AlN:Ho films. Both spectra give peaks at 362, 394, 461, 549, and 659 nm. These peaks correspond to $^5G_5 \rightarrow ^5I_8$, $^5G_4 \rightarrow ^5I_8$, $^5F_1 \rightarrow ^5I_8$, $^5S_2 \rightarrow ^5I_8$, and $^5F_3 \rightarrow ^5I_8$ transitions.²⁴ The dominant and highly intense peak at 549 nm gives green emission from Ho^{3+} . However the emission intensity changes when the films were thermally activated for 40 min at 1173 K. Increasing the temperature above 1300 K melted the optical fiber and hence our temperature (1173 K) is considered to be a suitable activation temperature. It was observed that thermal excitation enhances the intensity of the emission. Thermal activation has enhanced the intensity of 549 nm

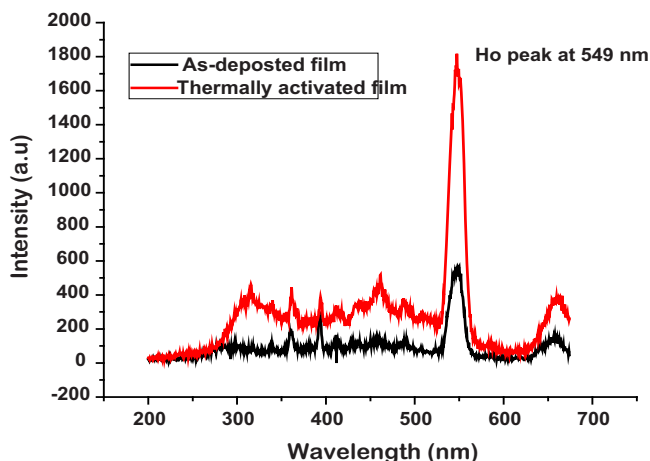


FIG. 6. (Color online) Luminescence spectra of AlN:Ho films before and after thermal activation.

peak more than the rest of the holmium peaks. It is clear from the figure that the intensity of green emission increases more than three times with thermal activation. This result is obtained by calculating the ratio of the 549 nm peak after thermal activation and before thermal activation. This tremendous increase in the intensity of the green emission from AlN:Ho with thermal activation is responsible for the fact that we can clearly see the green emission from the AlN:Ho doped optical fiber after thermal activation. Before thermal activation the intensity is not stronger enough to be seen directly.

The reason for such enhancement of the sample can be obtained by studying the physics behind this luminescence process. Luminescence occurs from Ho^{3+} ions and any Ho^{2+} or Ho^{1+} does not contribute to the emission. During the film deposition it is most likely that some of Al^{3+} of AlN may be replaced by Ho^{3+} . However, imperfections and defects can give rise to Ho^{2+} or Ho^{1+} during film growth, which cannot be ignored. The Ho^{2+} and Ho^{1+} ions do not contribute to luminescence. Smaller the number of these ions more will be Ho^{3+} and hence luminescence will be higher. When these films are activated thermally at a higher temperature then most of Ho^{2+} or Ho^{1+} impurities ionize and converts to Ho^{3+} ions giving path to enhanced luminescence.^{4,20–22} Moreover, when the films are transferred to the furnace and thermally annealed after removed from the deposition chamber and oxidized during the annealing process. This oxygen contamination cannot be ignored. The oxygen atoms enhance the luminescence of rare-earth ions, giving rise to the enhanced luminescence after thermal activation of the films.^{10,14,23}

The direct observation of green emission (Fig. 5) with naked eye explains that thermal annealing contributes to a tremendous enhancement in the luminescence from such rare-earth ions. This fact makes rare-earth ions very suitable candidates for photonic technology.

IV. CONCLUSION

In conclusion, thin films of holmium doped AlN were deposited on flat silicon substrates and optical fibers at liquid nitrogen temperature. AFM analysis shows that the as-deposited films on silicon substrate are amorphous but nanocrystals formation occurred in the thermally annealed films. All films on optical fiber were crystalline. Thermal annealing increases the intensity of the green emission from Ho^{3+} ions which can be observed with naked eye.

¹M. Maqbool, I. Ahmad, H. H. Richardson, and M. E. Kordesch, *Appl. Phys. Lett.* **91**, 193511 (2007).

²M. Maqbool and T. Ali, *Nanoscale Res. Lett.* **4**, 748 (2009).

³H. Chen, K. Gurumurugan, M. E. Kordesch, W. M. Jadwisienczak, and H. J. Lozykowski, *MRS Internet J. Nitride Semicond. Res.* **5**, U130 (2000).

⁴M. L. Caldwell, H. H. Richardson, and M. E. Kordesch, *MRS Internet J. Nitride Semicond. Res.* **5**, U142 (2000).

⁵W. M. Jadwisienczak, H. J. Lozykowski, F. Perjeru, H. Chen, M. Kordesch, and I. Brown, *Appl. Phys. Lett.* **76**, 3376 (2000).

⁶V. Dimitrova, P. G. Van Patten, H. H. Richardson, and M. E. Kordesch, *Appl. Phys. Lett.* **77**, 478 (2000).

⁷V. Dimitrova, P. G. Van Patten, H. H. Richardson, and M. E. Kordesch, *Appl. Surf. Sci.* **175–176**, 481 (2001).

⁸M. L. Caldwell, A. L. Martin, C. M. Spalding, V. I. Dimitrova, P. G. Van Patten, E. Martin Kordesch, and H. H. Richardson, *J. Vac. Sci. Technol. A* **19**, 1894 (2001).

- ⁹M. L. Caldwell, A. L. Martin, V. I. Dimitrova, P. G. Van Patten, M. E. Kordesch, and H. H. Richardson, *Appl. Phys. Lett.* **78**, 1246 (2001).
- ¹⁰M. L. Caldwell, P. G. Van Patten, M. E. Kordesch, and H. H. Richardson, *MRS Internet J. Nitride Semicond. Res.* **6**, 1 (2001).
- ¹¹H. H. Richardson, P. G. Van Patten, D. R. Richardson, and M. E. Kordesch, *Appl. Phys. Lett.* **80**, 2207 (2002).
- ¹²H. Chen, K. Chen, D. A. Drabold, and M. E. Kordesch, *Appl. Phys. Lett.* **77**, 1117 (2000).
- ¹³M. E. Little and M. E. Kordesch, *Appl. Phys. Lett.* **78**, 2891 (2001).
- ¹⁴M. Maqbool, H. H. Richardson, and M. E. Kordesch, *J. Mater. Sci.* **42**, 5657 (2007).
- ¹⁵J. B. Gruber B. Zandi, H. J. Lozykowski, and W. M. Jadwisienczak, *J. Appl. Phys.* **91**, 2929 (2002).
- ¹⁶J. F. Suyver, P. G. Kik, T. Kimura, A. Polman, G. Franzo, and S. Coffa, *Nucl. Instrum. Methods Phys. Res. B* **148**, 497 (1999).
- ¹⁷H. J. Lozykowski, *Phys. Rev. B* **48**, 17758 (1993).
- ¹⁸A. J. Steckl and R. Birkhahn, *Appl. Phys. Lett.* **73**, 1700 (1998).
- ¹⁹M. J. V. Bell, L. A. O. Nunes, and A. R. Zanatta, *J. Appl. Phys.* **86**, 338 (1999).
- ²⁰H. Jeong, S.-Y. Seo, and J. H. Shin, *Appl. Phys. Lett.* **88**, 161910 (2006).
- ²¹J. D. MacKenzie, C. R. Abernathy, S. J. Pearton, U. Hömmerich, J. T. Seo, R. G. Wilson, and J. M. Zavada, *Appl. Phys. Lett.* **72**, 2710 (1998).
- ²²S. Z. Wang, S. F. Yoon, L. He, and X. C. Shen, *J. Appl. Phys.* **90**, 2314 (2001).
- ²³M. Maqbool and I. Ahmad, *Curr. Appl. Phys.* **9**, 234 (2009).
- ²⁴M. Maqbool, M. E. Kordesch, and A. Kayani, *J. Opt. Soc. Am. B* **26**, 998 (2009).
- ²⁵S. V. Frolov, A. Fujii, D. Chinn, Z. V. Vardeny, K. Yoshino, and R. V. Gregory, *Appl. Phys. Lett.* **72**, 2811 (1998).
- ²⁶S. V. Frolov, Z. V. Vardeny, and K. Yoshino, *Appl. Phys. Lett.* **72**, 1802 (1998).
- ²⁷S. V. Frolov, M. Shkunov, Z. V. Vardeny, and K. Yoshino, *Phys. Rev. B* **56**, R4363 (1997).